Distributed UWB-based Ranging for Particle Tracking in Avalanches

Jonas Kuß*, Anselm Köhler†, Michael Neuhauser†, Rene Neurauter‡, Johannes Gerstmayr‡,
Jan-Thomas Fischer†, Falko Dressler*

*School of Electrical Engineering and Computer Science, TU Berlin, Germany
†Department of Natural Hazards, Austrian Research Centre for Forests, Austria
‡Department of Mechatronics, University of Innsbruck, Austria

`jonas.kuss@tu-berlin.de`, {`anselm.koehler, michael.neuhauser, jt.fischer`}`@bfw.gv.at`,
{`rene.neurauter, johannes.gerstmayr`}`@uibk.ac.at`, `dressler@ccs-labs.org`

Abstract—The inner dynamics and transport mechanisms of avalanches – especially on a particle level – remain hidden for most observation approaches. Knowledge of these processes is essential to develop and test analytical models that describe detailed processes in snow flows or the successful simulation of avalanche velocities and runouts. In this paper, we present a particle based, distributed tracking system that is based on ultra-wideband (UWB) ranging and localization. UWB-based positioning is particularly challenging in outdoor scenarios covering large distances in complex topography and fast moving, mobile systems. Our system model considers multiple anchor nodes distributed with inter-node distances in the order of a few hundred meters. Mobile nodes, which move with the avalanche in the field, are tracked via UWB measurements. We present our prototype and demonstrate through first experiments the general feasibility of UWB-based tracking in snow environments.

I. INTRODUCTION

Ranging and localization in dynamic outdoor environments is usually done using some global navigation satellite system (GNSS). While the technology is mature and has been very successful in many application domains, its main weaknesses are the comparably high energy consumption and the low accuracy in highly dynamic environments with complex toppography [1]. We are interested in one of such challenging environments, namely tracking the motion of snow avalanches in mountain areas on a particle level [2]. There is a strong need to investigate avalanche motion and their inner dynamics to validate and correct the data gathered from measurement efforts using sensing technologies such as radar, video analytics, inertial measurement units (IMUs), as well as simulation techniques [3]–[6].

The idea of the AvaRange measurement set-up is to introduce artificial particles of similar size and density to snow granules that are found in avalanches to track and reconstruct the trajectory of those transported particles to investigate the avalanche motion. First field experiments with measurement systems containing gyroscopes, magnetometers, and accelerometers led to promising results [2], [7], [8]. For radio ranging and localization, we focus on ultra-wideband (UWB), which allows very precise time-of-flight (ToF) measurements, which can also be used for angle-of-arrival (AoA) estimation and data
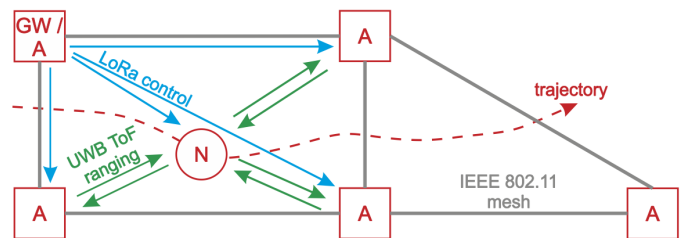

Figure 1. AvaRange system design: AvaAnchors (A) span an observation area. They are interconnected using an 802.11 mesh network. Gateways (GW) connect the system to our backend. AvaNodes (N) to be tracked use UWB for measurements and LoRa for configuration.

transmission following the joint communication and sensing (JCAS) principle.

UWB-based ranging has in general been well explored [9]–[11]. However, there are still many open questions related to outdoor environments covering larger distances; particularly with complex terrain and snow and ice conditions. Recently, some of the most popular UWB-based systems have been compared in indoor and outdoor scenarios [12]. At the same time, first measurements in snow (snow covered systems or communication through snow) [2], [13] confirmed the feasibility of UWB in our scenario.

In this paper, going beyond some initial observations [14], we introduce and discuss the AvaRange complete system architecture. Figure 1 depicts the conceptual system design. Anchors, called AvaAnchor, are deployed at the outline of the measurement area. The anchors use an IEEE 802.11 mesh in combination with LoRa for configuration and coordination of measurements. The objective is to provide ranging and eventually localization and tracking of nodes, called AvaNodes, moving in the measurement area. An UWB-based system is used for ToF measurements and the transport of these results via the anchors to a gateway node. The node is using the same UWB chip. The sensor housing is realized with varying shapes, sizes and densities in form of 3D-printed material, which are later placed in avalanche release areas and are transported with the gravitational mass flow.

We performed a set of experiments in an alpine area next to Innsbruck, Austria. Both experiments are done in

the experimental test site, which is used for the avalanche measurements. First, we present and discuss an winter, in-snow experiment to measure the impact of snow on the UWB ranging for sensors at rest and within simple motion. Additionally, we test the total reach and system accuracy within complex mountain terrain in a summer cable car experiment at the experimental test site to obtain a reproducible trajectory.

All results confirm the feasibility of our approach for the application within avalanche flow.

Our main contributions can be summarized as follows:

- We present a complete UWB-based radio ranging system for use in snow fields in mountain areas;
- we experimentally performed a set of initial experiments in a typical alpine region in the Alps; and
- we present results from these experiments confirming the envisioned measurement functionality.

II. RELATED WORK

Radio ranging techniques have been applied to various kinds of mass flows. Allan et al. [15] investigated simple received signal strength (RSS)-based methods with RFID tags in cobble stones to track their movement on sand and gravel beaches. Considering the very limited range of RFID transmitters this is not an option for our scenario.

In earlier work, we introduced the AvaRange concept. The idea is to rely on ToF radio ranging in combination with IMU to obtain accurate locations of a node being moved in an avalanche and to reconstruct the 3D trajectories. In this context, we also performed initial measurements in snow [2] and in the laboratory [8].

Vilajosana et al. [16] describe a conceptually similar approach. They use a TelosB sensor node equipped with a 2D accelerometer in combination with video recording and tested the system in a small scale artificial snow chute. The conclusion was that the electronics and sensors are basically suited for small scale measurements. Volkwein and Klette [17] apply a related approach to determine rockfall trajectories. They equip a block of rock with a microcomputer, sensors for translational and rotational movement, and an off-the-shelve 2D radio ranging appliance. However, they did not use the inertial data for trajectory reconstruction. Similarly, Caviezel et al. [18] developed the StoneNode, a low power sensor node that is used to conduct experiments to assess the forces occuring during rock fall.

UWB systems as used in our work have been extensively explored, particularly in indoor scenarios. For example, Jimenez and Seco [12] compared the popular Decawave and Bespoon UWB location systems, also considering a comparison between indoor and outdoor usage. First experimental results of UWB ranging errors in an outdoor environment have been presented by Kristem et al. [19]. Tightly coupled multi-sensor integration for seamless indoor and outdoor positioning using UWB has been studied by Jiang et al. [9]. Mobility aspects have been investigated more recently. For example, Mocanu and Onea [10] studied UWB-based localization for indoor and outdoor
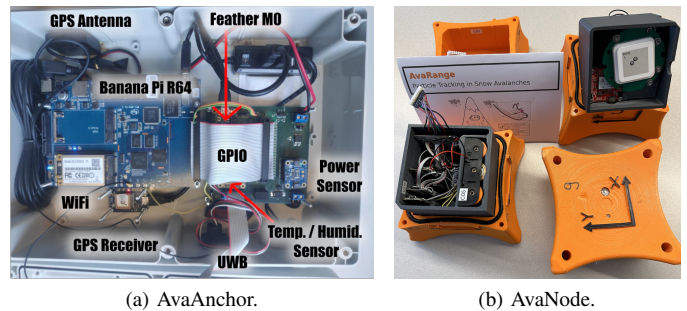

(a) AvaAnchor.

(b) AvaNode.

Figure 2. Core hardware systems used in our architecture. The heart of both the AvaAnchor and the AvaNode is a Arduino Feather M0 in combination with a DW1000 UWB chip for radio ranging. The AvaAnchor in addition uses a BananaPi for the WiFi mesh network.

vehicles; and Li et al. [11] used UWB ranging for localization in multi-robot systems.

Besides our initial study in 2016 [2], also Morales et al. [13] looked into using UWB as an airborne radar system for snow cover measurements, yet, the system does not support tracking of mobile particles.

III. SYSTEM DESIGN

A. System Architecture

The overall system concept is depicted in Figure 1. We distinguish three different device types. First, the mobile *node*, called AvaNode, represents the system to be tracked, i.e., the "particle" later on moving with the avalanche. Second, multiple *anchor* nodes, called AvaAnchors, are distributed along the tracking area. Both the AvaNode and the AvaAnchor are equipped with UWB-based ranging devices. One or multiple of the anchors are acting as a *gateway* device, which is used to coordinate measurements and to collect and forward experiment results to backend server systems.

For exchanging data, monitoring and controlling the system, and the ranging itself, we use a number of communication technologies. UWB is used by the DW1000 chip for the actual ranging procedure, i.e., ToF measurements. LoRa is used for sending commands to the node and transmitting sensor data at regular intervals. Anchors automatically create a 802.11 WiFi mesh network used for sending commands to anchors, setting ranging configurations, and transmitting ranging data to the backend server. WireGuard is used as a toolkit to integrate the mesh network. In addition, local GNSS receivers provide ground truth positions of the anchor nodes and absolute time.

B. AvaAnchor

A schematic overview of the AvaAnchor is depicted in Figure 2a. The main component is a BananaPi R64 running OpenWRT Linux for local processing. The BananaPi is connected to a custom PCB containing a Feather M0, a variety of sensors (e.g., temperature), and a DW1000 UWB chip for ToF radio ranging. The feather is responsible for collecting and transmitting sensor data such as temperature, humidity and power consumption. It also controls the power supply to the BananaPi, i.e., it is able to power-up / power-down
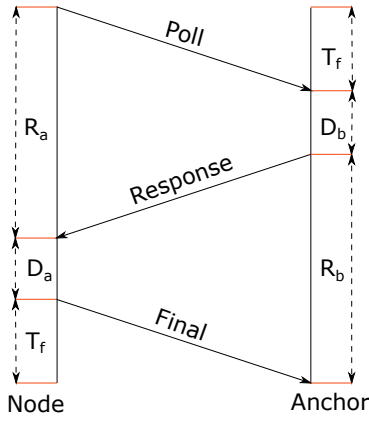
Figure 3. time-of-flight distance measurements between an anchor and the node based on transmission and reception timestamps obtained by the DW1000 USB chip.

the main system to save energy. A GNSS receiver is used to provide the position of the AvaAnchor and to support precise time synchronisation. The AvaAnchors contain an IEEE 802.11 WiFi card used to integrate them into an 802.11 mesh network for easy remote access, measurement configuration and transmission of measurement results. Selected AvaAnchors have an additional WiFi card. They act as gateways and are connected to an Internet uplink. The gateways control all other anchors and initiate UWB rangings. Of course, they also allow remote debugging and maintenance of all anchor systems via the mesh network.

C. AvaNode

The node is depicted in Figure 2b. For radio ranging, it also uses the same DW1000 UWB chip connected to an Arduino Feather M0. The DW1000 timestamping supports a precision of about $15\,\mathrm{ps}$,[1] which is essential for accurate ToF ranging. In addition, the AvaNode also includes a GNSS, an IMU, and recovery systems to locate and retrieve the AvaNodes after the experiments.

D. Ranging Procedure

To start an experimental run, i.e., to initiate a set of distance measurements between anchors and the node, participating anchors have to be powered on via a LoRa message sent from the gateway feather. After powering up the main system including the BananaPi, a DW1000 configuration is set on each anchor using the mesh network. Afterwards, the experimental run can be started and kept running by sporadically sending LoRa messages from the gateway feather to the mobile node containing a DW1000 configuration, an experiment name, and the number of rangings.

The ToF ranging procedure between an anchor and the node is depicted in Figure 3. We follow the ideas by Neirynck et al. [20] for the derivation of T_f, which is superior to normal double-sided ranging.

Both the anchor and the node always keep track of transmission and reception timestamps to calculate R_a, D_a, D_b, and R_b. The ranging is initiated by the node sending a poll message containing the experiment ID to the anchor. The anchor then answers with a reply message. The final message sent by the node contains both R_a and D_a. To calculate D_a, the exact sending timestamp has to be known before sending. This is not a problem, as the DW1000 supports a delayed sending mode, for which the sending timestamp is specified beforehand. The anchor can then calculate the ToF and consequently the distance as

$$T_f = \frac{R_a R_b - D_a D_b}{R_a + D_a + R_b + D_b}. \tag{1}$$

The approach can easily scaled to multiple anchors by sending the poll and final message as a broadcast, as well as assigning each anchor its own reply slot to prevent collisions. In general, to consistently trilaterate the position of the Node inside an avalanche, a minimum of four anchors have to be in range.

E. Measurement Data Post-Processing

When a single ranging is completed, each anchor stores information related to the ranging locally as well as in a remote sqlite and InfluxDB database for redundancy. This information consists of the following elements:

- Experiment name to map rangings to an experiment.
- Sequence number to store the order of rangings inside an experimental run.
- Ranging start and end to detect performance regressions.
- Node and anchor ID to identify ranging participants.
- Received signal strength indicator (RSSI) to estimate anchor orientation and distance accuracy.
- Calculated distance to the AvaNode.
- DW1000 configuration used in the experimental run.

For monitoring an ongoing ranging, we implemented a live representation of the measured data (as stored on the backend server) using a Grafana Dashboard.[2] Further analysis of the data and calculation of node positions after a completed experimental run is done using python scripts.

IV. Experiments and Results

A. In-Snow Experiment

We performed a set of in-snow measurements in a rather accessible terrain to evaluate the functionality of the system and to get initial insights on the measurement accuracy. The experiment site is located at the Nordkette, a mountain area in the Alps north of Innsbruck, Austria. Figure 4 shows the locations of the installed anchors as well as the positions of the measurements.

---

[1]DECAWAVE DW1000 Datasheet, https://www.decawave.com

[2]https://grafana.com/grafana/dashboards/
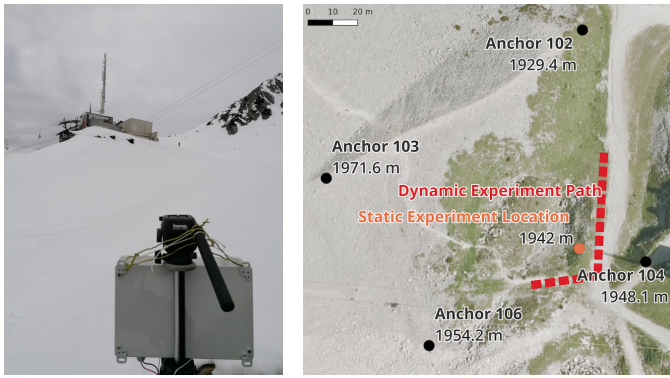
(a) Anchor at experiment site.   (b) Locations of anchors and experiments.

Figure 4. Winter experiment site at Nordkette, a mountain area in the Alps north of Innsbruck, Austria. The anchors were only reachable by experienced mountaineers. The locations of the anchors were chosen based on accessibility.
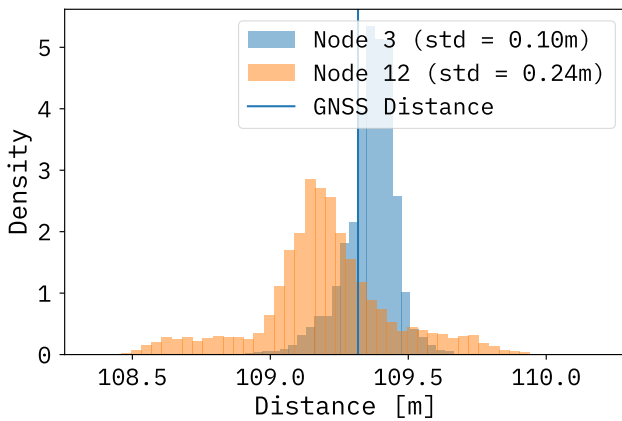

Figure 5. Ranging accuracy of in a stationary experiment. The histogram shows distribution of measurements for two nodes in different orientations towards Anchor 103. The vertical line depicts the ground truth distance as obtained by a high-precision GNSS.

1) Accuracy of UWB Rangings: We started the experiment series studying the UWB ranging accuracy of two stationary positioned nodes (cf. Figure 4b). Two different nodes were placed at the stationary location, with Node 3 facing upwards and Node 12 facing towards a 2 m deep wet snow ground layer. We also studied the effect of a snow cover between the nodes on the ranging. For this, we enclosed the nodes in layers of dry snow with varying thickness (2, 4 and 8 cm). To analyze the effect of snow water content, we also repeated the last experiment with wet snow, by gradually pouring water on top of the 8 cm thick snow cube.

Figure 5 shows a histogram of the ranging accuracy to one selected anchor, without any snow casing. We can see that the node orientation strongly impacts the ranging distribution, with Node 12 having more than double the standard deviation of Node 3. Also, Node 12 has some large distance errors of up to 80 cm, which are not present for Node 3.

We now investigate the impact of dry and wet snow on the ranging accuracy. We can see in Figure 6 that thicker layers
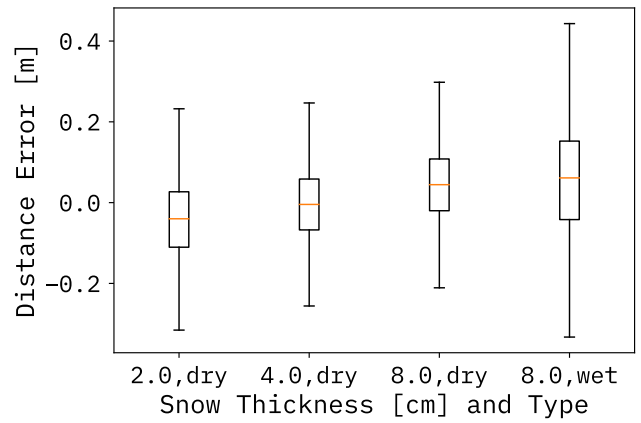

Figure 6. Impact of snow thickness and water content on the distance error. From left to right, we increase the thickness of the snow layer and finally add water for wet snow behavior.
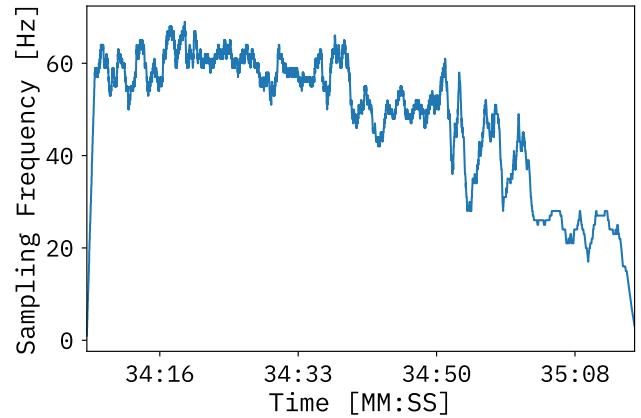

Figure 7. Impact of increased water content on ranging frequency. In this experiment, we slowly poured water on the dry snow while measuring the distance. Shown is the achievable sampling frequency over time.

of dry snow have no effect on ranging errors, but that a larger percentage of water in the snow decreases ranging accuracy significantly. So the cause for the large standard deviation in Figure 5 is not necessarily that Node 12 is facing towards the ground, but that the ground itself is comprised of wet snow.

In Figure 7, we can see that higher snow water content also decreases the number of successfully completed rangings significantly, to the point that rangings are no longer possible. This suggests that UWB ranging will be more effective, i.e., precise and frequent, for dry snow avalanches.

Finally, in Figure 8, we show the impact of the signal quality measured in form of the RSSI as reported by the DW1000 chip on the ranging accuracy. We show the dependency in form of a heat map. The results show that the signal is also strongly attenuated, particularly if snow is in between the sender and the receiver.
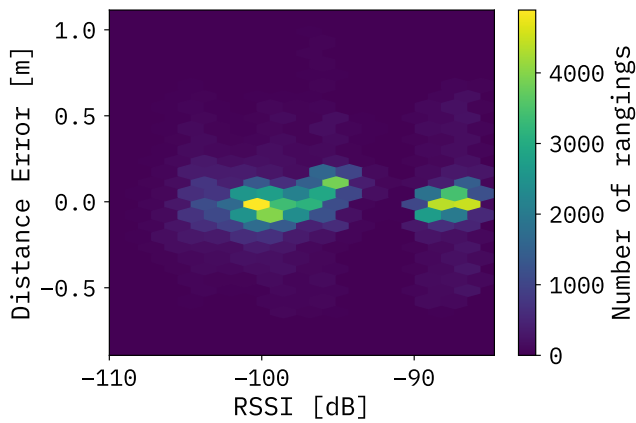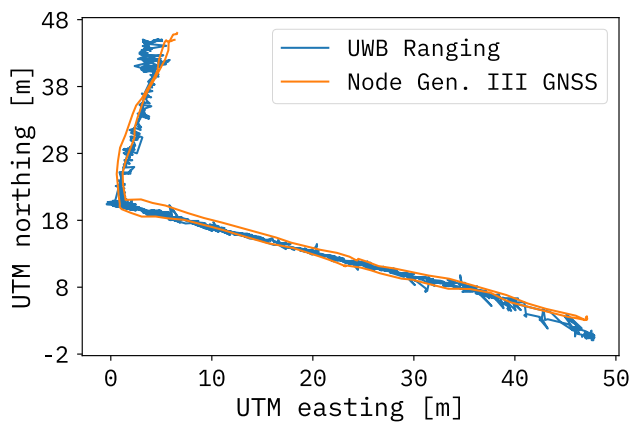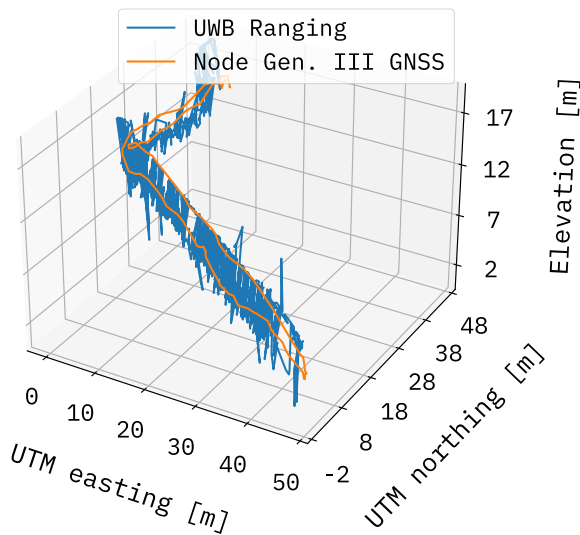
Figure 8. Impact of the signal strength measured in form of the RSSI on the ranging accuracy. The heat map shows the number of rangings as well as the distance error in relation to the RSSI.

(a) Mobile tracking in 2D

(b) Mobile tracking in 3D

Figure 9. Accuracy of the UWB-based ranging in a mobile scenario. A skilled skier took a node downhill. In order to get a ground truth, the skier also carried a high precision GNSS. As can be seen, the 2D accuracy is very high but the altitude measurement in 3D shows a higher degree of errors.

Figure 10. Equipment box fastened onto the cable car counterweight. The box contained both an AvaNode as well as a high precision GNSS system.

2) Tracking in a Mobile Scenario: In a second experiment, we explored the feasibility of tracking a mobile node. Instead of an avalanche, we had an experienced skier taking the node and skiing downhill, as exactly as possible following the track indicated in Figure 4b. In order to validate the measurement results, we also carried a separate high-precision GNSS tracker alongside the node. As can be seen in Figure 9, the accuracy of both systems is quite similar. We see that the 2D path matches the GNSS quite closely (cf. Figure 9a). Due to limited availability of anchors at this stage of the project, only rangings to three anchors were possible, leading to the large elevation differences in Figure 9b. So the 3D case can likely be improved by adding further anchors in this scenario.

One very important, and visually quite obvious, difference is the sampling rate. The UWB system can support a much higher sampling rate than the GNSS sensor. This will eventually impact the avalanche studies, as for dynamic measurements, the sampling frequency plays an enormous role to obtain most accurate information about the avalanche dynamics.

B. Cable Car Experiment

To evaluate the accuracy of our system and to compare against global navigation GNSS solutions, we conducted an experiment tracking the cable car of the local Innsbruck Nordkettenbahn which operates within the experimental test site, following the main trajectory of the corresponding avalanche path. For this, we mounted a box onto the cable car counterweight, which moves from the top towards the bottom cable car station (cf. Figure 10). The box contained a node with our UWB ranging system, a node with a uBlox Zed-F9P GNSS module and one high accuracy Emlid RTK GNSS for use as a reference. For the radio ranging, we placed six anchors in total; their reference locations were measured with the same Emlid RTK GNSS. Figure 11 shows the anchor locations along the cable car trajectory. Not shown is Gateway 101 at the valley station that provides the WiFi mesh uplink for all anchors.

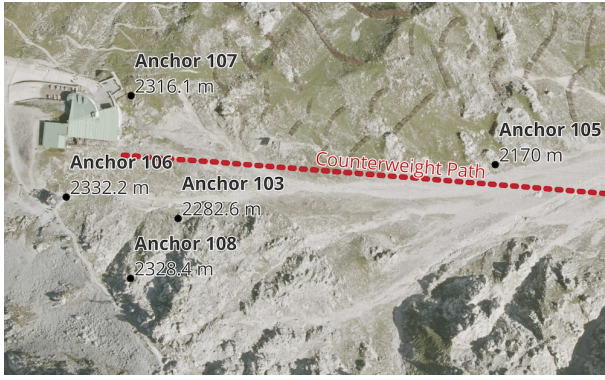Figure 12 shows the distance measurements collected by the respective anchors during the experiment. Depending on

Figure 11. Summer experiment site at Nordkette; a mountain area in the Alps north of Innsbruck, Austria. The anchors were placed along the trajectory of the cable car.
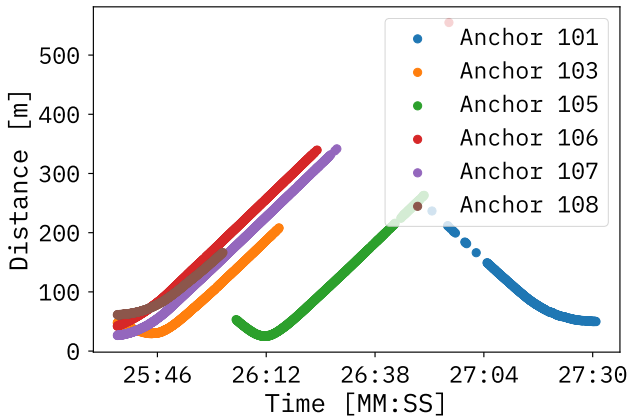

Figure 12. Distance measurements for the respective anchors over time for a single cable car ride. If at least 3 or 4 anchors provide distance measurements, 2D or 3D trilateration is possible, respectively.

Figure 13. Calculated 3D position of UWB-based tracking as well as the GNSS in our nodes compared to a high precision GNSS.

the orientation of the anchor towards the node, maximum achieved distance ranges from 200–300 m. As we need at least four distance measurements for 3D trilateration, The currently installed anchors cover about one third of the cable car route for successful trilateration.

Trilateration results are shown in Figure 13 in form of a 3D plot indicating the deviation from the path and in Figure 14 in form of a time series plot of the distance error compared to the reference. At the beginning, UWB ranging outperforms GNSS in precision. However, along the route the error increases in both variance and absolute value. The error is largest when the distance to all reachable anchors is largest. There is a small gap in time when less than three anchor nodes were reachable on the cable car trajectory.

The source of the inconsistencies in errors lies in the geometric dilution of precision (GDOP), which describes the effect of satellite geometry on expected position error. Before the measurement gap, rangings included all of the anchors at the top cable car station ({103, 106, 107, 108}). The further the node is along on the cable car route, the more narrow
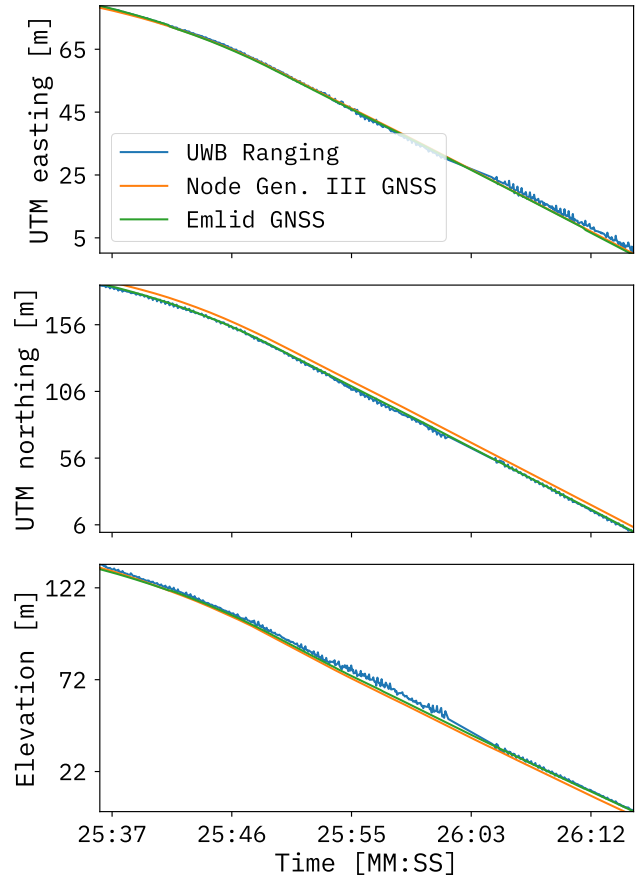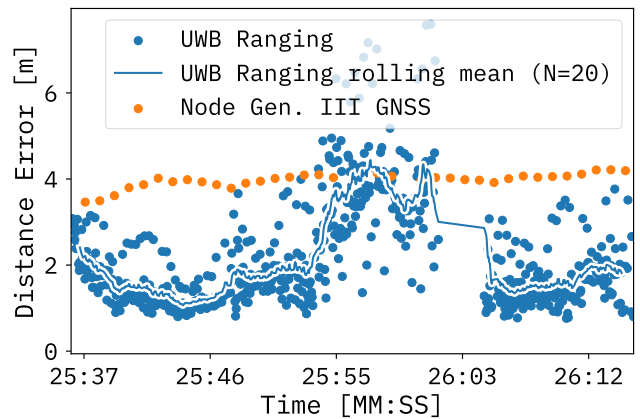

Figure 14. Absolute distance errors of UWB-based tracking compared to the high precision GNSS as a reference. For UWB, we plot both the single measurement points as well as a rolling mean.
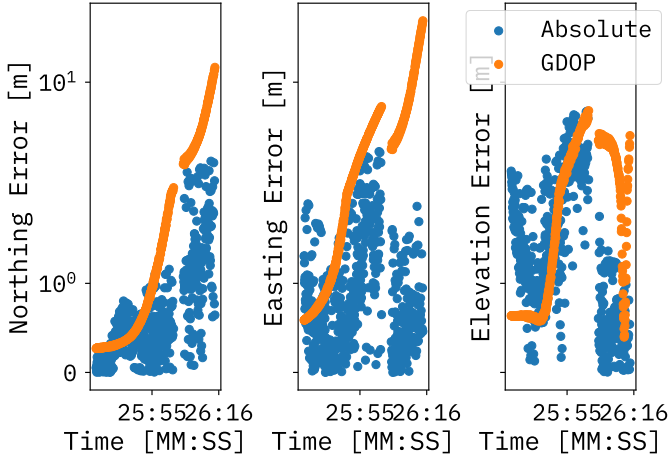
Figure 15. Comparison of GDOP with absolute errors compared to the high precision GNSS in all three dimensions.
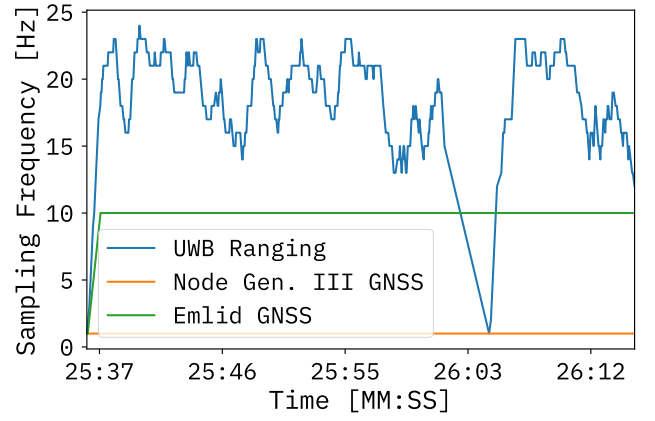

Figure 16. Sampling frequency of GNSS and UWB ranging. While the small form factor GNSS reports new positions at 1 Hz, the high precision GNSS has a frequency of 10 Hz. The UWB ranging is set to a measurement frequency of 25 Hz. Depending on radio connectivity, a sampling rate of 12–25 Hz can be achieved.

are the direction vectors towards the anchors around the top station. This effectively increases the intersection area of all the distance measurement circles and small errors in single distance components have a larger effect on the absolute position error. GDOP is calculated as

$$A = \begin{bmatrix} x_1 & y_1 & z_1 & 1 \\ x_2 & y_2 & z_2 & 1 \\ \ldots \\ x_i & y_i & z_i & 1 \end{bmatrix}$$

$$(A^T A)^{-1} = \begin{bmatrix} \sigma_x^2 & \sigma_x\sigma_y & \sigma_x\sigma_z & \sigma_x\sigma_t \\ \sigma_y\sigma_x & \sigma_y^2 & \sigma_y\sigma_z & \sigma_y\sigma_t \\ \sigma_z\sigma_x & \sigma_z\sigma_y & \sigma_z^2 & \sigma_z\sigma_t \\ \sigma_t\sigma_x & \sigma_t\sigma_y & \sigma_t\sigma_z & \sigma_t^2 \end{bmatrix} \cdot \frac{1}{\sigma_\tau^2}$$

where A is a matrix of all direction vectors from the node towards anchors a_i and σ_τ is the expected standard deviation of measurement error. For our use case, we can disregard the time dilution σ_t, as a single measurement only takes 40 ms to complete. As shown in Figure 5, we already determined $0.10\,\mathrm{m} \leq \sigma_\tau \leq 0.24\,\mathrm{m}$, depending on the orientation of the node towards the anchor.

Figure 15 shows a visualization of GDOP with a conservative estimate of $\sigma_\tau = 0.24\,\mathrm{m}$ in three dimensions. GDOP is able to track the error reasonably well in all dimensions. However, as the error differs in each measurement, GDOP can only estimate the expected error using σ_τ to some degree. Especially in the northing and easting axes, GDOP sometimes overestimates the error by a large amount, indicating that the distance error of these measurements is better than expected. But in general, GDOP value for the UWB ranging are accurate enough to indicate triangulation situations when the derived locations can eventually improved by sensor fusion techniques like Kalman filtering with integration of acceleration data from IMU sensors.

C. Discussion

All the shown results lead to the conclusion that we can be very satisfied with the performance and the achievable

maximum distances are beyond the datasheet. We expect dry snow in our experiments, thus, attenuation wont be too problematic. Of course, ranging improvements require more anchors and their positioning is crucial to minimize GDOP along the expected trajectory. As of now, we have not found a way to correlate single distance component errors with other data collected during the measurements, such as RSSI. So there is no way to reduce distance error for single measurements. Therefore, the only way to improve the absolute position error is to improve the position and number of anchors, such that the GDOP is minimized and the node is always able to reach at least four anchors. In the upcoming avalanche season, we will install more anchors for eventually measure full avalanche dynamics.

A clear advantage of our UWB-based ranging technique over GNSS is the much higher sampling rate. This mainly possible due to the smaller required measurement distances in the avalanche release area. The achievable sampling rate is shown in Figure 16. We are able to reach a sampling frequency between 15–25 Hz with UWB ranging, compared to the 1 Hz with GNSS. This allows us to detect sub-second changes in trajectory, which is especially important in avalanches, where the movement of the node will be more chaotic. Finally, only small form factor GNSS systems can be used in our avalanche nodes, which do not reach the accuracy and sampling frequency of high precision GNSS systems.

V. CONCLUSION

UWB-based ranging has meanwhile become a very mature technology. Still, from a practical perspective, many questions remain, which are often related to the overall localization system architecture and also to the coordination of measurements. In this paper, we presented the core concepts of our AvaRange measurement system, which allows to obtain fine-grained UWB measurements in large-scale outdoor environments. We

validated the system in the experimental test site, i.e., a mountain region in the Alps north of Innsbruck, Austria. In a winter experiment, we performed stationary experiments for calibration and to investigate the impact of snow in the line of sight between the UWB systems, as well as an experiment introducing mobility by having the node carried by an experienced skier.

From the results, we can see that our system is highly accurate in 2D with the majority of errors being less than 20 cm. The error in 3D is currently higher but this is the result of a limited number of anchor nodes at the moment. In a summer experiment, we compared our UWB ranging system with two GNSS-based systems. We particularly found a clear advantage in the sampling rate, which is more than one order of magnitude higher than with GNSS. Our system is at least as precise than a typical small form factor GNSS, provided that the anchors are positioned to achieve a good GDOP value. We also have to note that GNSS still provides better area coverage as we will need more permanently installed anchors to cover the complete avalanche release area. In a next step, we plan for dynamic measurements in the next avalanche season.

REFERENCES

[1] X. Li, M. Ge, X. Dai, X. Ren, M. Fritsche, J. Wickert, and H. Schuh, "Accuracy and reliability of multi-GNSS real-time precise positioning: GPS, GLONASS, BeiDou, and Galileo," *Journal of Geodesy*, vol. 89, no. 6, pp. 607–635, Mar. 2015.

[2] F. Erlacher, B. Weber, J.-T. Fischer, and F. Dressler, "AvaRange - Using Sensor Network Ranging Techniques to Explore the Dynamics of Avalanches," in *12th IEEE/IFIP Conference on Wireless On demand Network Systems and Services (WONS 2016)*, Cortina d'Ampezzo, Italy: IEEE, Jan. 2016, pp. 120–123.

[3] T. Faug, B. Turnbull, and P. Gauer, "Looking Beyond the Powder/Dense Flow Avalanche Dichotomy," *Journal of Geophysical Research: Earth Surface*, vol. 123, no. 6, pp. 1183–1186, Jun. 2018.

[4] C. Ligneau, B. Sovilla, and J. Gaume, "Numerical investigation of the effect of cohesion and ground friction on snow avalanches flow regimes," *PLOS ONE*, vol. 17, no. 2, e0264033, Feb. 2022.

[5] B. Reuter, L. Viallon-Galinier, S. Horton, A. van Herwijnen, S. Mayer, P. Hagenmuller, and S. Morin, "Characterizing snow instability with avalanche problem types derived from snow cover simulations," *Cold Regions Science and Technology*, vol. 194, p. 103 462, Feb. 2022.

[6] J.-T. Fischer, M. Neuhauser, A. Köhler, F. Oesterle, A. Wirbel, O. Dick, W. Fellin, R. Winkler, R. Neurauter, J. Gerstmayr, J. Kuß, and F. Dressler, "On the potential of particle tracking in snow avalanches," in *International Snow Science Workshop (ISSW 2023)*, Bend, OR, Oct. 2023, pp. 48–55.

[7] M. Neuhauser, A. Köhler, R. Neurauter, M. S. Adams, and J.-T. Fischer, "Particle trajectories, velocities, accelerations and rotation rates in snow avalanches," *Annals of Glaciology*, pp. 1–18, Oct. 2023.

[8] R. Neurauter, A. Holzinger, M. Neuhauser, J.-T. Fischer, and J. Gerstmayr, "Motion Reconstruction of Fast-rotating Rigid Bodies," *Journal of Computational and Nonlinear Dynamics*, pp. 1–15, Nov. 2023.

[9] W. Jiang, Z. Cao, B. Cai, B. Li, and J. Wang, "Indoor and Outdoor Seamless Positioning Method Using UWB Enhanced Multi-Sensor Tightly-Coupled Integration," *IEEE Transactions on Vehicular Technology*, vol. 70, no. 10, pp. 10 633–10 645, Oct. 2021.

[10] R. Mocanu and A. Onea, "Indoor and Outdoor Vehicle Localization using UWB Transceivers," in *27th IEEE Mediterranean Conference on Control and Automation (MED 2019)*, Acre, Israel: IEEE, Jul. 2019, pp. 299–303.

[11] M. Li, Z. Chang, Z. Zhong, and Y. Gao, "Relative Localization in Multi-Robot Systems Based on Dead Reckoning and UWB Ranging," in *23rd IEEE International Conference on Information Fusion (FUSION 2020)*, Rustenburg, South Africa: IEEE, Jul. 2020, pp. 1–7.

[12] A. Jimenez and F. Seco, "Comparing Decawave and Bespoon UWB location systems: Indoor/outdoor performance analysis," in *IEEE International Conference on Indoor Positioning and Indoor Navigation (IPIN 2016)*, Alcalá de Henares, Spain: IEEE, Oct. 2016, pp. 1–8.

[13] F. R. Morales, C. Leuschen, C. Carabajal, A. Wolf, and S. Garrison, "Measurements of snow cover using an improved UWB 2-18 GHz airborne radar testbed," in *IEEE Radar Conference (RadarConf 2018)*, Oklahoma City, OK: IEEE, Apr. 2018, pp. 1033–1036.

[14] J. Kuß, A. Köhler, M. Neuhauser, J.-T. Fischer, R. Neurauter, J. Gerstmayr, and F. Dressler, "A Measurement System for Distributed UWB-based Ranging and Localization in Snow Avalanches," in *29th ACM International Conference on Mobile Computing and Networking (MobiCom 2023), Poster Session*, Madrid, Spain: ACM, Oct. 2023.

[15] J. C. Allan, R. Hart, and J. V. Tranquili, "The use of Passive Integrated Transponder (PIT) Tags to Trace Cobble Transport in a Mixed Sand-and-Gravel Beach on the High-energy Oregon coast, USA," *International Journal of Marine Geology, Geochemistry and Geophysics*, vol. 232, no. 1, pp. 63–86, Oct. 2006.

[16] I. Vilajosana, J. Llosa, M. Schaefer, E. Surinach, and X. Vilajosana, "Wireless sensors as a tool to explore avalanche internal dynamics: Experiments at the Weissfluehjoch Snow Chute," *Cold Regions Science and Technology*, vol. 65, no. 2, pp. 242–250, Feb. 2011.

[17] A. Volkwein and J. Klette, "Semi-Automatic Determination of Rockfall Trajectories," *Sensors*, vol. 14, no. 10, pp. 18 187–18 210, Sep. 2014.

[18] A. Caviezel, M. Schaffner, L. Cavigelli, P. Niklaus, Y. Bühler, P. Bartelt, M. Magno, and L. Benini, "Design and Evaluation of a Low-Power Sensor Device for Induced Rockfall Experiments," *IEEE Transactions on Instrumentation and Measurement*, vol. 67, no. 4, pp. 767–779, Apr. 2018.

[19] V. Kristem, S. Niranjayan, S. Sangodoyin, and A. F. Molisch, "Experimental determination of UWB ranging errors in an outdoor environment," in *IEEE International Conference on Communications (ICC 2014)*, Sydney, Australia: IEEE, Jun. 2014.

[20] D. Neirynck, E. Luk, and M. McLaughlin, "An alternative double-sided two-way ranging method," in *13th Workshop on Positioning, Navigation and Communications (WPNC 2016)*, Bremen, Germany: IEEE, Oct. 2016.